Catalysis Letters 57 (1999) 221–226

Time-resolved Eu luminescence spectra and kinetics at various Y zeolitic environments

Sunbae Lee, Hanshin Hwang, Pilseok Kim and Du-Jeon Jang *

Department of Chemistry and Research Institute of Molecular Science, Seoul National University, Seoul 151-742, Korea
E-mail: djjang@plaza.snu.ac.kr

Received 7 October 1998; accepted 11 January 1999

Time-resolved spectra and kinetic profiles as well as static spectra of Eu luminescence are measured to understand the binding site characteristics and migration of catalytically important metal cations in Y zeolite. As calcination temperature increases, stoichiometrically exchanged Eu^{3+} ions, initially hydrated at indefinite sites in the supercage, pass through site II′ to migrate into sites I and I′ first and the remnants, after binding at sites I and I′, stay at site II′.

Keywords: Y zeolite, Eu luminescence, cation binding, catalysis, cation migration

1. Introduction

Zeolites have been extensively investigated [1–4] as they play indispensable roles in many technological and economical applications. Zeolites are known to dispense various unusual catalytic effects on encapsulated chemical species [5–7]. Many of their catalytic properties are related to acidic and basic properties which depend on the cations they contain [2,3]. The modification of zeolites by exchanging cations [2,8,9] is a useful method of tailoring their properties to particular applications. Especially, the presence of rare-earth cations is reported to improve their thermal stability and catalytic activity [2,8,10]. Improvement would be optimized with understanding the environment of cations and their interactions with neighbors.

Highly luminescent properties of rare-earth cations are extensively utilized to solve a variety of structural and analytical problems [11–16] as their spectra, quantum yields, and lifetimes are sensitive to environment. In particular, Eu luminescence is remarkably valuable. Excitation to the strongly allowed $^5L_6$ level from the ground $^7F_0$ level leads the Eu^{3+} ion to the $^5D_0$ level by means of fast nonradiative relaxation processes at room temperature, prior to radiative relaxation to one of the ^7F_J ($J = 0$–6) levels (figure 1). Mainly monitored luminescence bands in this report are the transition bands of $^5D_0 \rightarrow {}^7F_1$, $^5D_0 \rightarrow {}^7F_2$, and $^5D_0 \rightarrow {}^7F_4$ and they will be called F_1, F_2, and F_4, respectively. The electric dipole transition of F_2 is forbidden by parity in symmetry with an inversion center [17,18]. However, interactions with the ligand field or with vibrational states mix electronic states of different parities and the transition [17,19] arising from this hybridization is called forced electric dipole transition. As the forced transition of F_2 originates from interactions with neighbors, it is hypersensitive to, especially short-range, environmental effects [19–21]. F_4 is also an electric dipole transition and is sensitive to long-range environmental effects [19–21]. However, the magnetic dipole transition of F_1 is allowed and insensitive to the surroundings of the Eu^{3+} ion so that it is usually utilized as an internal standard [19,22]. For example, if RI(2), the ratio of F_2 luminescence intensity to F_1 intensity, is larger, the binding site of the Eu^{3+} ion has lower symmetry and less polar and more covalent character [19]. A larger RI(4), the ratio of F_4 intensity to F_1 intensity, implies an increased long-range interaction of the Eu^{3+} ion with its surroundings [19].

In this report, we present time-resolved and static Eu luminescence spectra measured at various Y zeolitic environments. The results reveal the characteristics of Eu^{3+} binding sites in Y zeolite and the migration of Eu^{3+} ions

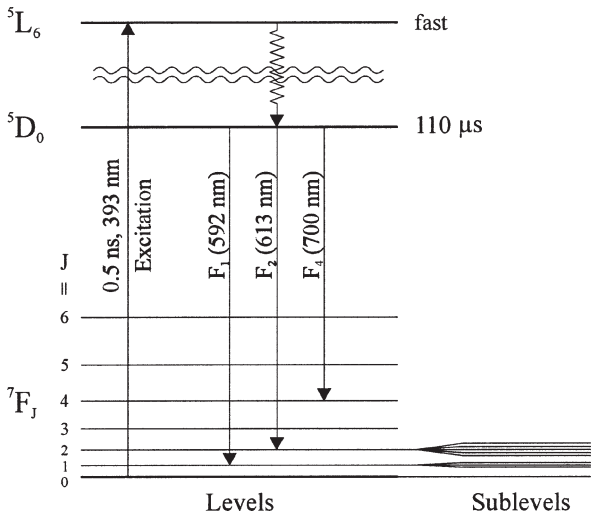

Figure 1. Schematic energy levels and relaxation dynamics of aqueous Eu^{3+} at RT to show the transitions of excitation and mainly monitored luminescence bands.

* To whom correspondence should be addressed. Also a member of the Center for Molecular Science, Taejon 305-701, Korea.

among binding sites with calcination progress, suggesting that Eu luminescence spectroscopy is an excellent probe into cation binding sites.

2. Experimental

Eu^{3+}-exchanged Y zeolite (EuY) was prepared by refluxing synthesized Na^{+}-exchanged Y zeolite (NaY) in stoichiometrically (2.7 Eu^{3+} ions per supercage) concentrated aqueous solution of $EuCl_3 \cdot 6H_2O$, purchased from Aldrich, at 70–80 °C for a day. Refluxed zeolite was filtered, dried in a desiccator overnight and then transferred into a glass-jointed quartz tube of 6 mm inner diameter under nitrogen atmosphere. The tubed sample was further dehydrated and calcined at a desired temperature under vacuum of 10^{-2} Torr for 6 h until the glass entrance of the tube was sealed off with a torch. However, dehydrated samples still contain a great number of hydrated water molecules. About 20 water molecules are still found to be hydrated per unit cell even when samples are calcined at 450 °C [2]. Deuterated samples were prepared by treating the above refluxing procedure in ^2H_2O. The sample temperature during spectral measurement was controlled with a closed-cycle helium refrigerator (Janis Research, CCS-100). Unless specified otherwise, all zeolite samples were refluxed in ^1H_2O and calcined at 400 °C, and all spectral measurements were carried out at room temperature (RT).

Static luminescence spectra were measured by using a home-made fluorometer, which consists of a 350 W Xe lamp (Schoeffel, LPS255HR), 0.25 m excitation (Kratos, GM252) and 0.275 m emission (Acton Research, Spectrapro275) monochromators, and a PMT (Hamamatsu, R926). All the static and time-resolved luminescence spectra reported here were measured from front surface excitation at 393 nm and not corrected for the wavelength-dependent variation of detector sensitivity. Samples were excited with 0.5 ns pulses from a dye laser (Laser Photonics, LN102) pumped by a nitrogen laser (Laser Photonics, LN1000) for time-resolved spectra and decay kinetic profiles. Luminescence was focused into a 0.5 m spectrometer (Acton Research, Spectrapro500) which was coupled with an intensified CCD (Princeton Instruments, ICCD-576-G) for time-resolved spectra, while it was collected into a 0.25 m monochromator (Bausch & Lomb, 33-86-79) attached with a PMT (Hamamatsu, R928) for kinetic profiles (figure 2). Time-resolved spectra from the CCD controller and kinetic profiles from a digital oscilloscope (Tektronix, TDS350) appended to the PMT were accumulated and averaged with a 586 PC computer. The relative trigger times between the laser and the detectors were adjusted with a delay/pulse generator (Standford Research Systems, DG535).

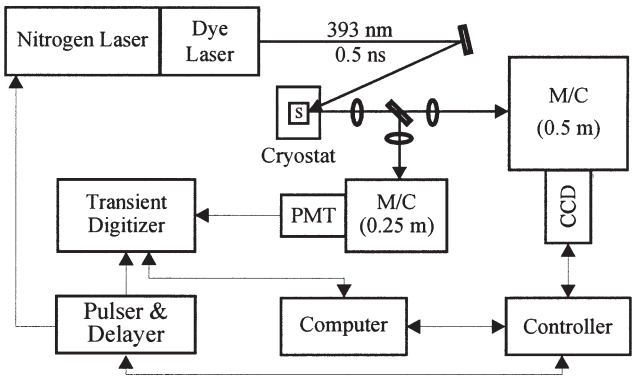

Figure 2. Schematic diagram of experimental setup.

3. Results and discussion

Figure 3 shows that the static Eu luminescence spectrum of EuY is quite different from that of Eu^{3+} aqueous solution, but also that it varies significantly with temperature. The relative intensities of the F_2 and F_4 bands increase dramatically with binding to the zeolite so that they are even much larger than that of the F_1 band. The fact that the RI(2) value of Y zeolite in table 1 is eight times as big as that of aqueous solution indicates that the Eu^{3+} binding sites of Y zeolite have much lower symmetry and less polar and more covalent characters than water. Notwithstanding the reduced overall polarity of immediate neighbors compared with water, an increased long-range interaction, suggested from the increment of RI(4) by three times, implies that zeolite is more crystalline, as known, and that it has locally distributed strong ionic groups. As both short- and long-range interactions with neighbors decrease, both

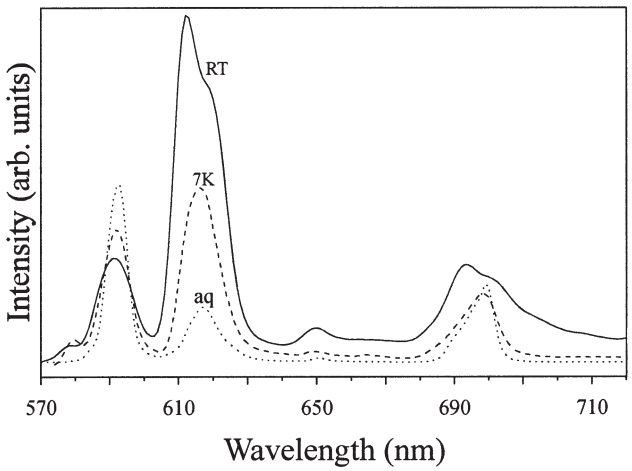

Figure 3. Luminescence spectra, normalized by F_1 band areas, of EuY at RT (RT), EuY at 7 K (7K), and aqueous Eu^{3+} solution at RT (aq). Note that the relative intensities of F_2 and F_4 bands vary enormously depending on Eu^{3+} ion environment.

Table 1
RI values of the spectra in figure 3.

Sample (temperature)	Aqueous solution (RT)	Y zeolite (RT)	Y zeolite (7 K)
RI(2)	0.5	4.0	1.8
RI(4)	0.6	1.9	0.8
RI(2)/RI(4)	0.9	2.1	2.1

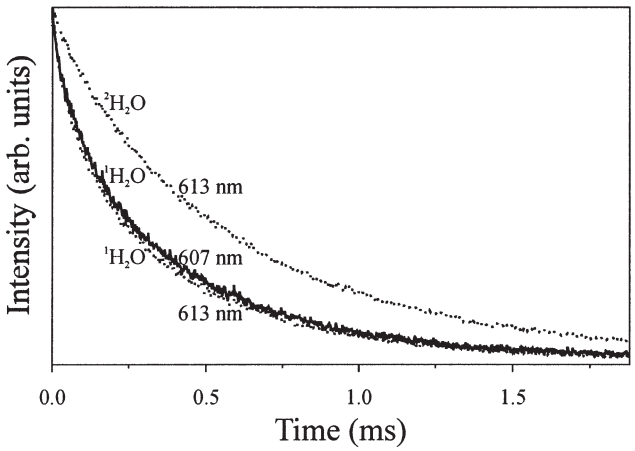

Figure 4. Luminescence decay kinetic profiles of EuY. The refluxed solvents and monitored wavelengths are shown near the respective profiles.

Table 2
Decay time constants obtained from the profiles in figure 4.

Sample	λ_{em} (nm)	Decay time constant (μs)
Refluxed in ^1H_2O	607	150 (49%) + 600 (51%)
Refluxed in ^1H_2O	613	150 (54%) + 600 (46%)
Refluxed in ^2H_2O	613[a]	340 (53%) + 910 (47%)

[a] The water coordination numbers calculated from the decay time constant variations with hydrogen isotope exchange are 3.9 and 0.6 for the fast and slow components, respectively.

RI(2) and RI(4) become smaller at a temperature as low as 7 K (table 1). It is interesting to note that the ratio of RI(2)/RI(4) remains the same regardless of a large temperature change. This invariance results from the unchangeableness of the crystalline zeolite framework with temperature variation [23].

The luminescence decay profile of EuY calcined at 400 °C fits well into a double exponential decay with decay times of 150 and 600 μs, although the overall decay kinetics and the relative amplitudes of the two components depend on collected emission wavelengths (figure 4 and table 2). Since luminescence components with different time constants are expected to originate from different environments, we have tried to understand the surroundings of the individual components by measuring decay time variations with hydrogen isotope exchange [24,25] and by examining spectral change with time. As residually existing hydrated water in the surface of the calcined sample is exchanged with heavy water, the fast and slow decay time constants are altered into 340 and 910 μs, respectively, with no considerable changes in relative amplitudes. The numbers of water molecules coordinated to a Eu^{3+} ion, estimated following the method of Horrocks and Subnick [24], are 3.9 and 0.6 for the fast and slow decay components, respectively. Considered that an aqueous Eu^{3+} ion has 8–9 coordinated water molecules in the aspect of luminescence quenching dynamics [24,26], the actual numbers of coordinated water molecules might be lower than the observed ones. Nevertheless, the Eu^{3+} site responsible for the fast decay is located apparently much closer to hydrated water molecules than the site for the slow decay.

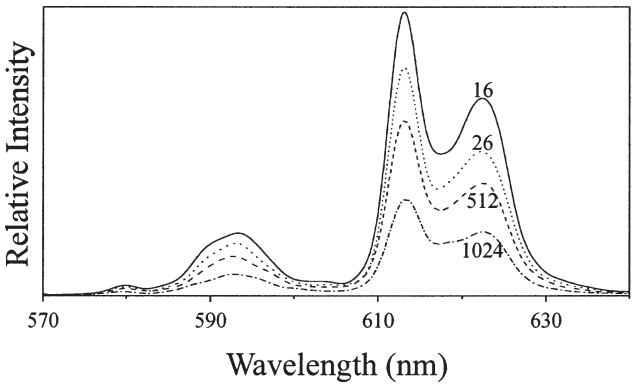

Figure 5. Time-resolved luminescence spectra of EuY at different delay times (μs) from sample excitation.

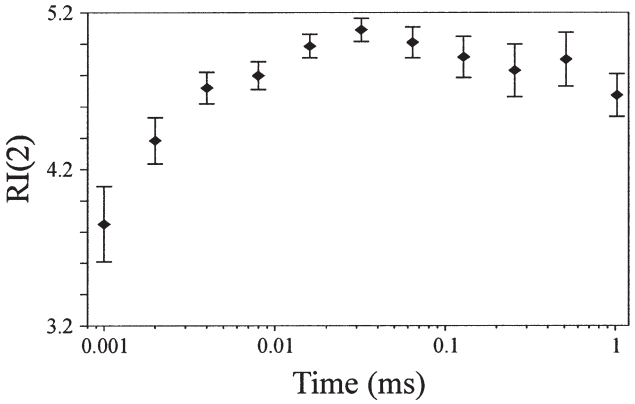

Figure 6. RI(2) variation with delay time.

Any meaningful changes such as spectral shift may not be noticeable at a glance into the time-resolved spectra of figure 5 owing to rather a slight spectral change with time. Nonetheless, the calculated RI(2) value in figure 6 increases at early time and remains steady with delay time, denoting that the slower decay component with a high RI(2) is emitted from sites with lower symmetry and more covalent character. We have examined the hypersensitive F_2 band in figure 7 to look into any spectral changes with delay time. Assuming that the spectral bands of two decay components are linearly combined with different relative amplitudes at different delay times to give time-resolved spectral bands, we have deconvoluted the spectral contours of two decay components in figure 7(b) from the time-resolved spectra at 16 and 1064 μs in figure 7(a). Compared with the fast band, the slow one has a broader bandwidth with a shallower dip near 617 nm and is shifted to the blue. The broader bandwidth signifies less definite location, suggesting that the slow decaying luminescence may be brought about from more than one sites with slightly different characters. The overall blue shift also supports a more covalent environment suggested by the larger RI(2) of the slow band.

The hypersensitive F_2 band of EuY changes spectrally quite significantly with calcination temperature variation

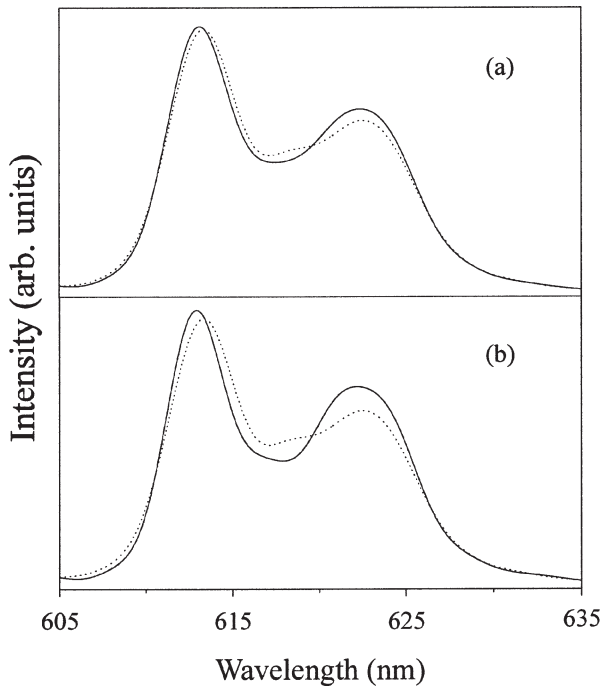

Figure 7. (a) Area-normalized F_2 bands at the delay times of 16 μs (solid) and 1064 μs (dotted) and (b) fast (solid) and slow (dotted) decay components deconvoluted from the two.

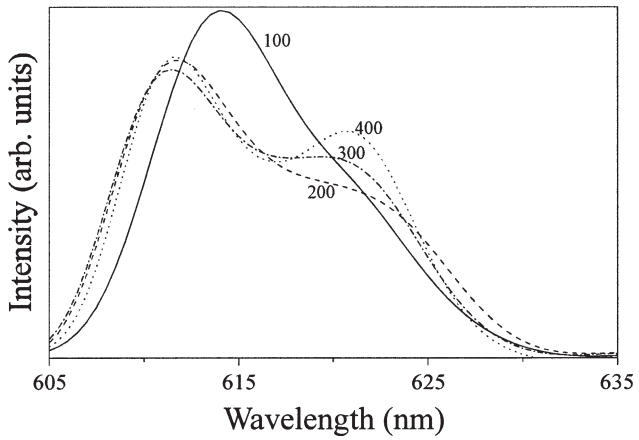

Figure 8. Area-normalized F_2 spectra of EuY dehydrated at various temperatures (°C).

Table 3
Peak wavelengths and spectral band widths of the spectra in figure 8.

	Calcination temperature (°C)			
	100	200	300	400
λ_{max} (nm)	614.0	611.6	611.4	611.4
fwhm (nm)	10.8	14.7	15.4	15.1

(figure 8 and table 3). With calcination temperature increase the peak emission wavelength shifts to the blue until 300 °C and then remains the same, while the spectral bandwidth increases until 300 °C and then decreases. These facts indicate that Eu^{3+} ions migrate into environmentally diverse binding sites with overall less polarity as

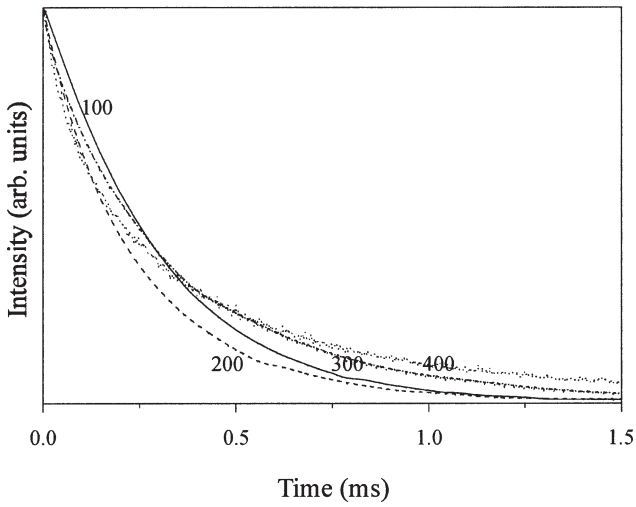

Figure 9. Luminescence decay kinetic profiles at 613 nm of EuY dehydrated at various temperatures (°C).

Table 4
Decay time constants obtained from the profiles in figure 9.

Calcination temperature (°C)	Decay time constant (μs)
100	290
200	290 (65%) + 150 (35%)
300	290 (59%) + 150 (15%) + 600 (26%)
400	150 (54%) + 600 (46%)

hydrated water molecules disappear with calcination temperature increase until 300 °C. Above 300 °C the spectral bandwidth decreases with calcination temperature increment as Eu^{3+} ions move somewhat easily to bind to energetically stable sites only, rather than kinetically easily accessible metastable sites. The fact that the spectrum of the sample calcined at 100 °C is similar in shape to the spectrum of aqueous Eu^{3+} in figure 3, with a slight shift to the blue by 5.0 nm, suggests that Eu^{3+} ions are hydrated at indefinite sites when dehydrated at 100 °C. As the calcination temperature increases, the depression near 617 nm becomes more easily noticeable, expressing an increase in the number of sublevels with temperature rise. The number of sublevels for the F_2 band at one binding site is known to increase from one up to five as the symmetry of the binding site decreases from the icosahedral group [17]. Thus the increase of sublevels implies that the overall symmetry of binding sites becomes lower with calcination progress.

The calcination temperature dependence of Eu luminescence decay profile and time constants (figure 9 and table 4) reveals well that Eu^{3+} ions migrate from one site to another as calcination moves onward with temperature rise. When the sample was calcined at 100 °C, the profile fits into a single exponential decay with the time constant of 290 μs. Together with the F_2 band spectrum that looks like the spectrum from aqueous solution, the single decay fit suggests that the most strongly interacting neighbors of Eu^{3+} ions are hydrated water molecules in spite of preliminary dehydration, although the blue shift of the peak

wavelength by 5.0 nm and the significantly enlarged lifetime of 290 from 110 μs indicate that Eu^{3+} ions are not fully hydrated and that they are bound to sites less polar than water. Although La^{3+} ions in hydrated faujasite zeolites are found [2] to exist at sites II′, II and IV, the characteristics of specific Eu^{3+} binding sites are not revealed with the Eu luminescence probe for the sample calcined at 100 °C, as luminescence characteristics are mostly determined by strongly interacting hydrated water molecules. The site IV mentioned above is the location within the large aperture leading to the supercage. The cation binding site in the hexagonal prism is called site I. However, there are two cation sites in the sodalite cage. The one near site I is called site I′, while the other located close to the supercage is site II′. The profile from the sample prepared at 400 °C shows a double exponential decay with the fast and slow components presented in figure 4 and table 2. The profile of the sample dehydrated at 200 °C shows biphasic decay times of 290 and 150 μs. However, the profile from the sample calcined at 300 °C is intentionally fitted to a triphasic exponential decay with the time constants of 290, 150, and 600 μs to find their relative amplitudes. These calcination temperature-dependent variations suggest that Eu^{3+} ions migrate from one site to another as dehydration proceeds with calcination temperature elevation. Furthermore, it should be noted that the relative amplitude of the fast component increases at first and then decreases as the relative amplitude of the slow component starts to increase. After Eu^{3+} ions bind stoichiometrically completely to the site responsible for the slow component, then they bind to the site of the fast component. These migration differences unveil that the relatively kinetically easily accessible site accords with the fast component, while the energetically stable site with the slow one.

Eu luminescence from dehydrated EuY decays biphasically with the lifetimes of 150 and 600 μs. The relative amplitudes of the two components are about the same. The fast and slow decaying components are emitted from Eu^{3+} ions coordinated with 3.9 and 0.6 water molecules, respectively. Relatively, the slow component is spectrally broader and shifted to the blue and it has a larger RI(2) value. This suggests that the slow component originates, relatively, from a more covalent environment distant from the hydrated surface of the supercage and from a less definite location with lower symmetry. Considering these results, we allocate the site II′ for the location of Eu^{3+} emitting the fast component and the sites I′ and I for the location of Eu^{3+} emitting the slow component. A unit cell of La^{3+}-exchanged hydrated Y zeolite is reported [27] to have 13.1, 16.0, and 29.1 La^{3+} ions at sites I, I′, and II′, respectively. The one stable location of site II′ agrees with the narrower spectral width of the fast component and the two similar but different locations of sites I′ and I go with the broader F_2 band of the slow component. The cation site of supercage near site II′ is called site II and contains 30 Na^+ ions for each unit cell of hydrated NaY zeolite, while sites I and I′ bear 7.5 and 19.5 Na^+ ions, respectively [28]. The more ionic environment of site II′ also goes well with the smaller RI(2) and red shift of the fast component. The shorter lifetime and larger water coordination number of the fast component also suggest much easier interaction of excited Eu^{3+} at site II′ with water molecules hydrated at the polar location of site II.

In hydrated samples the different characteristics of individual Eu^{3+} binding sites are not disclosed well, as Eu luminescence attributes are mostly determined by strongly interacting coordinated water molecules. As hydrated water molecules are largely located at supercage surfaces in hydrated Y zeolite [2,23], Eu^{3+} ions should be hydrated at indefinite sites in the supercage as well. As La^{3+} ions and water molecules are found mainly at sites II′ and II after an initial dehydration [2,23,27], it is considered that Eu^{3+} ions start to migrate into site II′ above 100 °C. However, Eu^{3+} ions migrate further to fill sites I and I′ stoichiometrically at a high temperature above 300 °C and then to bind site II′ stoichiometrically, for the sites I and I′ are relatively more difficult to access kinetically but stronger to bind Eu^{3+} ions. As reported that most water molecules are located at site II′ for the samples dehydrated above 400 °C [23], the luminescence from site II′ decays much faster than that from sites I′ and I.

4. Conclusions

Time-resolved and static results from EuY zeolite show that Eu luminescence spectroscopy is an excellent site-selective probe into the surroundings of catalytically important metal cations in zeolites. Stoichiometrically exchanged Eu^{3+} ions, initially hydrated at indefinite sites in the supercage of Y zeolite, pass through site II′ to migrate into sites I and I′ as dehydration proceeds with calcination temperature rise. After binding at sites I and I′ stoichiometrically, the remnant ions migrate to fill site II′. Eu luminescence from site II′ decays fast as in 150 μs owing to interaction with hydrated water molecules existent after calcination at 400 °C, while that from sites I′ and I decays in the time scale of 600 μs. The slow decaying luminescence is, relatively, spectrally broader and shifted to the blue and shows a larger RI(2) value.

Acknowledgement

We thank Professor Ryong Ryoo at the Center for Molecular Science for his kind gift of Y zeolite. This work was supported by the Korea Science and Engineering Foundation (961-0305-083-2). DJ also acknowledges the Hallym Academy of Sciences, Hallym University and the Korea Ministry of Education.

References

[1] W. Chen, Z.G. Wang, Z.J. Lin and L.Y. Lin, Solid State Commun. 101 (1997) 371.

[2] K. Gaare and D. Akporiaye, J. Phys. Chem. B 101 (1997) 48.
[3] S. Takatani, H. Fukumura and H. Masuhara, J. Phys. Chem. B 101 (1997) 3365.
[4] H.-M. Kao and C.P. Grey, J. Phys. Chem. 100 (1996) 5105.
[5] K.B. Yoon, Y.S. Park and J.K. Kochi, J. Am. Chem. Soc. 118 (1996) 12710.
[6] V. Ramamurthy, J. Am. Chem. Soc. 116 (1994) 1345.
[7] V. Ramamurthy, D.R. Sanderson and D.F. Eaton, J. Phys. Chem. 97 (1993) 13380.
[8] C. Stolz, A. Sauvage, P. Massiani and R. Kramer, Appl. Catal. A 167 (1998) 113.
[9] M.D. Baker, M.M. Olken and G.A. Ozin, J. Am. Chem. Soc. 110 (1988) 5709.
[10] T. Bada, S. Hikita, Y. Ono, T. Yoshida, T. Tanaka and S. Yoshida, J. Mol. Catal. A 98 (1995) 49.
[11] T. Yamase, T. Kobayashi, M. Sugeta and H. Naruke, J. Phys. Chem. A 101 (1997) 5046.
[12] K. Fujita, K. Tanaka, K. Hirao and N. Soga, J. Appl. Phys. 81 (1997) 924.
[13] G. Pucker, K. Catterer, H.P. Fritzer, M. Bettinelli and M. Ferrari, Phys. Rev. B 53 (1996) 6225.
[14] T. Tanaka, T. Yoshida, S. Yoshida, T. Baba and Y. Ono, Physica B 208–209 (1995) 687.
[15] M. Rizk, Y. El-Shabrawy, N.A. Zakhari, S.S. Toubar and L.A. Carreira, Spectrosc. Lett. 28 (1995) 1235.
[16] J. Reuben, *Handbook on the Physics and Chemistry of Rare Earths* (North-Holland, Amsterdam, 1979) p. 515.
[17] J.-C.G. Bunzli, in: *Lanthanide Probes in Life, Chemical and Earth Sciences*, eds. J.-C.G. Bunzli and G.R. Choppin (Elsevier, Amsterdam, 1989) ch. 7.
[18] F. Bergaya and H. van Damme, J. Chem. Soc. Faraday Trans. 79 (1983) 505.
[19] E.W.J.L. Oomen and A.M.A. van Dongen, J. Non-Cryst. Solids 111 (1989) 205.
[20] L.D. Carlos and A.L.L. Videira, Phys. Rev. B 49 (1994) 11721.
[21] F.S. Richardson, Chem. Rev. 82 (1982) 541.
[22] D. Levy, R. Reisfeld and D. Avnir, Chem. Phys. Lett. 109 (1984) 593.
[23] P. Norby, F.I. Poshni, A.F. Gualtieri, J.C. Hanson and C.P. Grey, J. Phys. Chem. B 102 (1998) 839.
[24] W.D. Horrocks, Jr. and D.R. Subnick, Acc. Chem. Res. 14 (1981) 384.
[25] Y. Haas and G. Stein, J. Phys. Chem. 76 (1972) 1093.
[26] W.D. Horrocks, Jr. and D.R. Subnick, J. Am. Chem. Soc. 101 (1979) 334.
[27] D.W. Breck, *Zeolite Molecular Sieves: Structure, Chemistry, and Use* (Wiley, New York, 1974) p. 100.
[28] J.M. Bennet and J.V. Smith, Mater. Res. Bull. 3 (1968) 633.